UDK 629.4.023

INVESTIGATION OF HEAT TRANSFER COEFFICIENTS FOR PASSENGER CAR BODY FENCING USING A CONTROLLED TEST ENVIRONMENT

KAMOLIDDIN INOYATOV [0000-0002-1502-8642]

Tashkent State Transport University, 1 Temiryulchilar Str., Tashkent 100069, Uzbekistan

Abstract. *This study investigates the thermal performance of passenger car body enclosures using a controlled test chamber. Due to the relatively high heat transfer coefficient of existing designs, the need for improved thermal insulation has been identified. Modern insulation materials with low thermal conductivity were analyzed, and four prototype samples were tested. The best results were obtained from samples using corundum and polyurethane foam. These materials also provide effective corrosion protection. To ensure measurement accuracy, the test chamber was calibrated. The study presents a validated methodology for selecting thermal insulation materials for railway rolling stock.*

Keywords: *heat transfer coefficient, passenger car, insulation, test chamber, corundum, polyurethane foam.*

To determine the heat transfer coefficient of the thermal fences of the body of a passenger car, not enough research has been carried out so far. The heat transfer coefficient of the passenger car body is K = 1,0-1,1 W/m^2·K [1]. This is a fairly high value. Consequently, the car body enclosure needs to improve the thermal insulation properties, taking into account the choice of thermal insulation materials with a low thermal conductivity coefficient [2-10].

In this work, modern thermal protective materials for fencing the car body, having the lowest thermal conductivity coefficients, were analyzed and prototypes of the body fencing in the test chamber were tested.

In view of the fact that part of the heat flux generated by the heat is dissipated into the environment, and the measurement of heat flux through the structure under study is difficult, it has been proposed to use a closed chamber in the form of a parallelepiped with replaceable upper covers.

The test chamber is a closed chamber made of sheet foam with a thermal conductivity of λ = 0,028 W/m·K. Figure 1 shows a general view of the chamber showing the thicknesses of its elements (side walls, bottom and cover). The test chamber with temperature sensors (2 units) and a heating element (P = 15W) are located inside the refrigeration chamber, the control panel is located outside the refrigeration chamber. To improve accuracy, three graduated covers were made of the same material from the same delivery, but of different thicknesses: δ_1 = 40 mm, δ_2 = 60 mm, δ_3 = 80 mm.

The average area of the chamber is determined by the formula:

$$F_{av} = \sqrt{F_{ext} \cdot F_{int}}, \quad (1)$$

where F_{av} – average camera area, m^2; F_{ext} – outer surface area of the chamber, m^2; F_{int} – interior chamber volume, m^2.

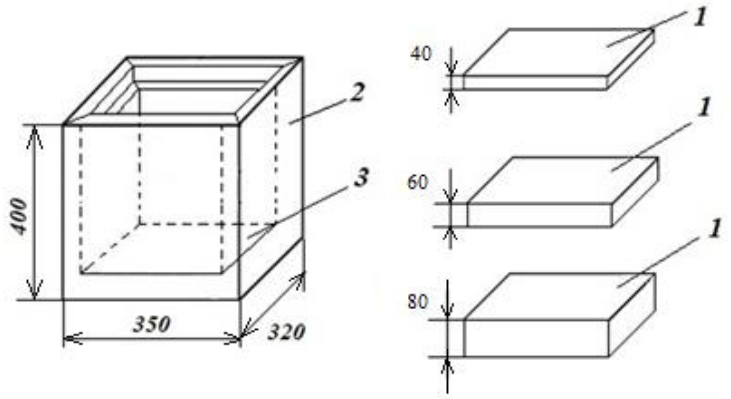

Fig. 1. General view of the test chamber: 1 – cover; 2 – side walls; 3 – bottom

Table 1 – Results of calculation of chamber elements areas

№	Camera elements	F_{ext}, m^2	F_{int}, m^2	Average area, m^2	F_{cam}, m^2
1	Side walls 1, 3	0.14	0.076	0.103	0.384
2	Side walls 2, 4	0.128	0.064	0.09	0.386
3	Bottom	0.112	0.030	0.057	0.057
4	Cover	0.064	0.030	0.043	0.043
5	Average chamber area, F_n	-	-	-	0.486
6	Average area of the chamber without cover, F_{un}	-	-	-	0.443

The task of calibration of the test chamber is to determine the heat transfer coefficient F_{cam} of the test chamber using three removable covers. The temperature inside the test chamber was maintained between 10 ºC and 62 ºC with an outside temperature of 10 ºC and 52 ºC with an outside temperature of -10 ºC by means of a XH-W1209 thermostat, so that the temperature difference t_{int} - t_{ext} was maintained at 52 ºC with an interval ± 0.5 ºC. According to the experiment, a graph of temperature t ˚C in the test chamber and electricity consumption W was plotted.

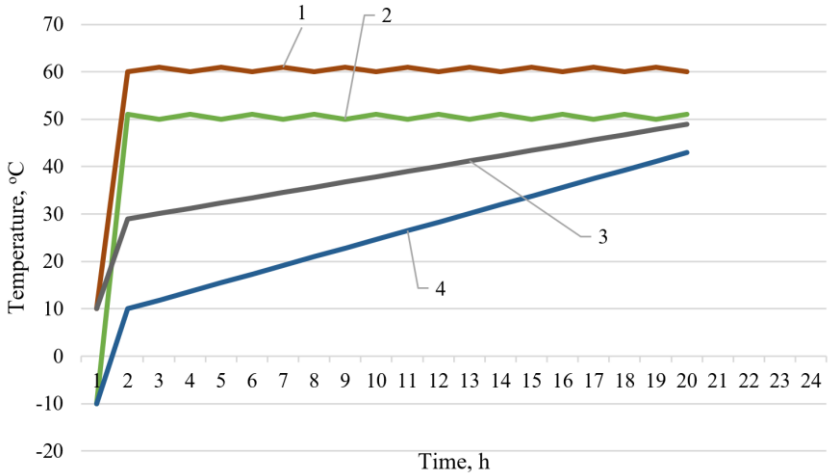

Fig. 2. – Diagram of temperature in the test chamber and power consumption: 1 – temperature in the chamber at t_{ext}=10 ºC; 2 – temperature in the chamber at t_{ext}= - 10 ºC and 52˚C and t_{int}=62 ºC; 3, 4 – power consumption

The graph (figure 2) shows that the steady-state mode takes from 2 to 2.5 hours, that is, at this time the thermostat provides constant power to heat the interior of the test chamber until the steady-state heat transfer mode occurs. The heating of the chamber stops every 0.5 ºC, when turned on, it

heats up, heat is transferred from the inside of the chamber to the outside through the elements of the chamber.

Since the chamber elements are made of the same material (foam), heat transfer will occur through all the chamber elements (side walls, bottom and cover).

To separate the heat transfer through the cover and the chamber body (side walls and bottom), we use the Fourier law formula based on the Newton-Richman law [7].

$$\frac{Q}{F} = \frac{\delta}{\lambda}(t_{in} - t_{ex}), \quad (2)$$

where Q – specified heat flow, W/s; F – cross-sectional area through which heat is transferred, m^2; λ – thermal conductivity coefficient, W/m·K; δ – material thickness, m; t_{in} and t_{ex} – wall surface temperature, K.

Based on the results of the experiment, the total heat transfer coefficient of the chamber K_f can be determined by the formula [8]:

$$K_f = \frac{W}{F_{av} \cdot \tau \cdot (t_{in} - t_{ex})}, \quad (3)$$

where K_f – heat transfer coefficient of the whole chamber, W/(m^2·K); W – power consumption for the design measurement period, W·h; F_{av} – geometric mean value of the chamber area, m^2; τ – time of the calculation period, h; t_{ext} – average ambient air temperature, ºC; t_{int} – average air temperature inside the chamber, ºC; (t_{int}-t_{ext}) – average temperature difference inside and outside during the measurement period, ºC.

The heat transfer coefficient of test covers is calculated by the formula [9-13]:

$$K_{lid} = \frac{1}{\frac{1}{\alpha_{int}} + \frac{\delta}{\lambda} + \frac{1}{\alpha_{ext}}} \quad (4)$$

As a result of calculations, we obtain the value of the coefficient of the cover with a thickness of 80 mm – 0,250 W/m^2·K, covers with a thickness of 60 mm – 0,330 W/m^2·K, covers with a thickness of 40 mm – 0,480 W/m^2·K.

To calculate the heat transfer coefficient of the body of the KK chamber without covers, we will use the formula:

$$K_f \cdot F_f = K_{sw} \cdot F_{sw} \cdot 4 + K_{bott} \cdot F_{bott} + K_{lid} \cdot F_{lid}\,, \quad (5)$$

where K_f – is the heat transfer coefficient of the test chamber as a whole, determined experimentally by formula (3); K_{sw}, K_{bott}, K_{lid} – heat transfer coefficients of side walls, bottom and roof; F_f, F_{sw}, F_{bott}, F_{lid} – average areas of the entire chamber, side walls, bottom and cover.

Formula (5) is written as follows

$$K_f \cdot F_{sw} = \frac{4K_{sw} \cdot F_{sw} + K_{bott} \cdot F_{bott} + K_{lid} \cdot F_{lid}}{F_{sw} + F_{bott} + F_{lid}}\,. \quad (6)$$

To simplify formula (6), we denote $4K_{sw} \cdot F_{sw} + K_{bott} \cdot F_{bott}4$ as $K_{fr} \cdot F_{fr}$ and F_{sw}+F_{bott} as F_{lid} we get the formula in the form

$$K_f = \frac{K_{fr} \cdot F_{fr} + K_{lid} \cdot F_{lid}}{F_{fr} + F_{lid}}\,, \quad (7)$$

we write formula (7) as

$$K_f \cdot F_{fr} + K_f \cdot F_{lid} = K_{fr} \cdot F_{fr} + K_{lid} \cdot F_{lid}. \quad (8)$$

From formula (8) we can find the value of the coefficient of the chamber body K_{fr}

$$K_{fr} \cdot F_{fr} = \frac{K_f \cdot F_{fr} + K_f \cdot F_{lid} - K_{lid} \cdot F_{lid}}{F_{fr}};$$

or

$$K_{fr} = \frac{K_f \cdot (F_{fr} + F_{lid}) - K_{lid} \cdot F_{fr}}{F_{fr}}\,. \quad (9)$$

There are two unknowns, K_{fr} and K_{lid}, in formula (9). But we know by formula (4) the heat transfer coefficients of the calibration covers.

$$K_{lid}^{80} = 0{,}250 \text{W/m}^2\text{·K},\ K_{lid}^{60} = 0{,}330 \text{ W/m}^2\text{·K},\ K_{lid}^{40} = 0{,}480 \text{ W/m}^2\text{·K}.$$

We enter the ratios of the coefficients of the covers 40, 60 through the value of the cover 80.

$$K_{lid}^{40} = 1{,}92 \cdot K_{lid}^{80}\,; \qquad K_{lid}^{60} = 1{,}32 \cdot K_{lid}^{80}\,.$$

Given these relations, we compose the equations for the three caps

$$K_{fr}^{80} = \frac{K_f \cdot (F_{fr}+F_{lid}) - K_{lid}^{80} \cdot F_{lid}}{F_{fr}},$$
$$K_{fr}^{60} = \frac{K_f \cdot (F_{fr}+F_{lid}) - 1{,}32 \cdot K_{lid}^{80} \cdot F_{lid}}{F_{fr}}, \quad (10)$$
$$K_{fr}^{40} = \frac{K_f \cdot (F_{fr}+F_{lid}) - 1{,}92 \cdot K_{lid}^{80} \cdot F_{lid}}{F_{fr}}.$$

Solving equations (10), we obtain the values of the heat transfer coefficient of the chamber body K_{fr}. Calculations showed that the heat transfer coefficient of the test chamber body has an average value of K_{fr} = 0.492 W/m^2·K.

The difference between the three K_{fr} values is 1.5-2%. The calculation results are summarized in table 2.

Thus, the heat transfer coefficient of the body of the test chamber is obtained for calibrating the chamber and can be used to determine the heat transfer coefficients of prototypes of the body fence in combination with further experiments.

Table 2 – Test chamber calibration results

№	Parameter	Cover, mm		
		δ = 80	δ = 60	δ = 40
1	Average cover area F_{fr}, m^2	0.043	0.043	0.043
2	Average area of the chamber without cover, F_{fr}, m^2	0.443	0.443	0.443
3	Total average area of the test chamber, F_{av}, m^2	0.486	0.486	0.426
4	Heat transfer coefficient of covers, W/m^2 K	0.250	0.330	0.480
5	Experiment power consumption, W	217	221	238
6	Chamber assembly heat transfer coefficient at expirations K_f, W/m^2·K	0.426	0.456	0.496
7	Chamber body heat transfer coefficient K_{fr}, W/m^2·K	0.482	0.495	0.501

Experimental studies of prototypes of body fencing. The metal frame of the body is solid. Side walls represent a frame including upper and lower straps, vertical posts and longitudinal elements of *Z*-shaped profile. The roof of the car consists of lower binding, transverse curved arcs and longitudinal elements of a Z-shaped profile. Steel plate 2 and 2.5 mm thick shall be used for external cladding. After assembly, the frame is covered with a primer. Recesses between transverse and longitudinal elements are filled with heat insulation. The inner skin is plastic 2 mm thick. Side and end walls have openings for windows and doors. As the basic design of the car, a stopped car with a length of 23.6 m was adopted. In this work, the thermal fencing of the side walls and roofs is considered. Longitudinal and transverse elements form cells in which heat insulation materials are placed. Requirements for heat-shielding materials shall comply with OSJD standards (rules O + P538/1). Thermal insulation of the car body.

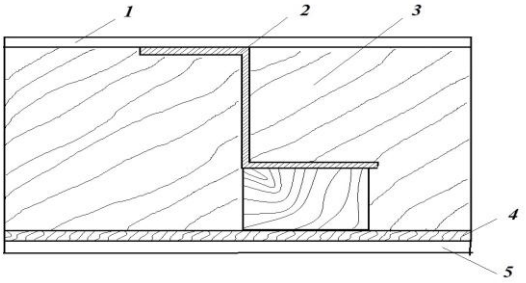

Fig. 3. – General view of body heat insulation

For experiments, 5 samples of thermal insulation were made. Each sample is a model of thermal insulation of the body measuring 270x240 mm. Sample №1 - calibration, consists of three covers,

samples № 2, 3, 4, 5 are models of experimental structures of thermal insulation of the body (table 3).

Table 3 – Sketches of test fencing samples

<table>
<tr><th>Sample sketch</th><th>Material and its parameters</th></tr>
<tr><td colspan="2">Sample №1</td></tr>
<tr><td> 
</td><td>Calibration samples of covers with thickness;
δ=80 mm λ=0,028 W/m·K
δ=60 mm λ=0,028 W/m·K
δ=40 mm λ=0,028 W/m·K
material-penoplex</td></tr>
<tr><td colspan="2">Sample №2</td></tr>
<tr><td> 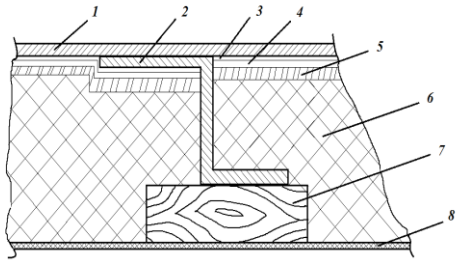
</td><td>
<table>
<tr><th>Material</th><th>δ, m</th><th>λ, W/m·K</th></tr>
<tr><td>1-steel</td><td>0.002</td><td>46.2</td></tr>
<tr><td>2-steel</td><td>0.003</td><td>46.2</td></tr>
<tr><td>3-emlak</td><td>0.0005</td><td>0.016</td></tr>
<tr><td>4-izomast</td><td>0.003</td><td>0.18</td></tr>
<tr><td>5-ceramics</td><td>0.003</td><td>0.15-0.2</td></tr>
<tr><td>6-izover</td><td>0.080</td><td>0.041</td></tr>
<tr><td>7-tree</td><td>0.04</td><td>0.02-0.2</td></tr>
<tr><td>8-plastic</td><td>0.0015</td><td>0.2</td></tr>
</table>
</td></tr>
<tr><td colspan="2">Sample №3</td></tr>
<tr><td> 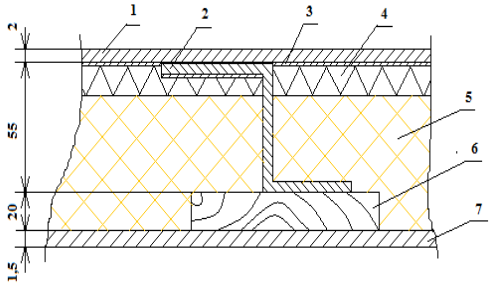
</td><td>
<table>
<tr><th>Material</th><th>δ, m</th><th>λ, W/m·K</th></tr>
<tr><td>1-steel</td><td>0.002</td><td>46.2</td></tr>
<tr><td>2-steel</td><td>0.004</td><td>46.2</td></tr>
<tr><td>3-corundum</td><td>0.0015</td><td>0.0012</td></tr>
<tr><td>4-polyurethane</td><td>0.03</td><td>0.04</td></tr>
<tr><td>5-penopleks</td><td>0.025</td><td>0.028</td></tr>
<tr><td>6-tree</td><td>0.020</td><td>0.08</td></tr>
<tr><td>7-plastic</td><td>0.0015</td><td>0.2</td></tr>
</table>
</td></tr>
<tr><td colspan="2">Sample №4</td></tr>
<tr><td> 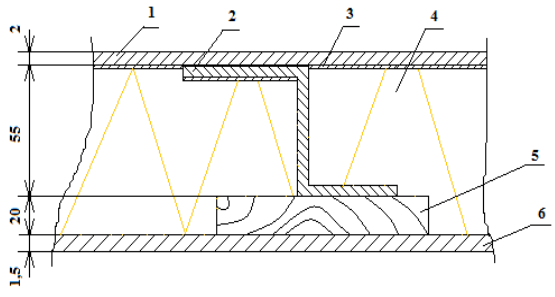
</td><td>
<table>
<tr><th>Material</th><th>δ, m</th><th>λ, W/m·K</th></tr>
<tr><td>1-steel</td><td>0.002</td><td>46.2</td></tr>
<tr><td>2-steel</td><td>0.003</td><td>46.2</td></tr>
<tr><td>3-corundum</td><td>0.0015</td><td>0.0012</td></tr>
<tr><td>4-polyurethane</td><td>0.052
0.072</td><td>0.046</td></tr>
<tr><td>5-tree</td><td>0.020</td><td>0.23</td></tr>
<tr><td>6-plastic</td><td>0.0015</td><td>0.2</td></tr>
</table>
</td></tr>
<tr><td colspan="2">Sample №5</td></tr>
<tr><td></td><td>
<table>
<tr><th>Material</th><th>δ, m</th><th>λ, W/m·K</th></tr>
<tr><td>1-steel</td><td>0.002</td><td>46.2</td></tr>
</table>
</td></tr>
</table>

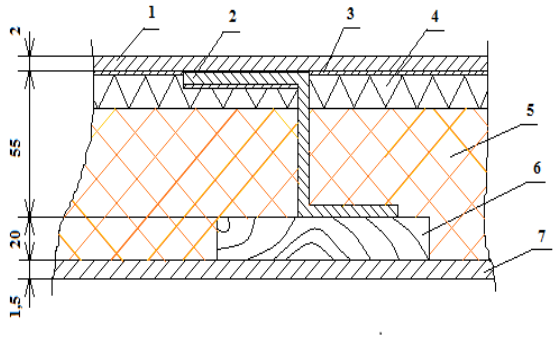

2-steel	0.003	46.2
3-corundum	0.0015	0.0012
4-polyurethane	0.052 0.072	0.046
5-izover	0.028	0.041
6-tree	0.020	0.23
7-plastik	0.0015	0.2

Fig. 4. – Prototype frame: 1 – sheathing sheet; 2 – *Z*-shaped profile

Figure 5 shows prototypes of the fence. Samples №2, 3, 4 and 5 are based on steel sheet δ = 2 mm thick and *Z*-shaped profile №5.

a

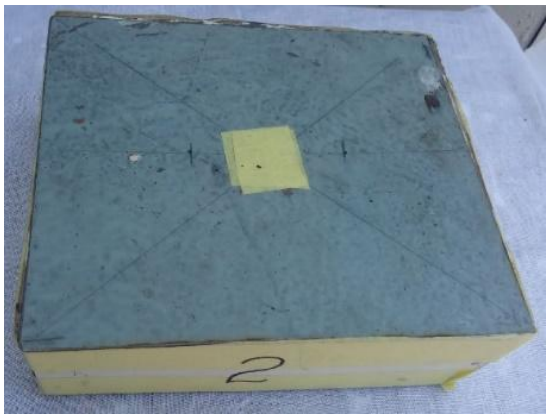

b

c

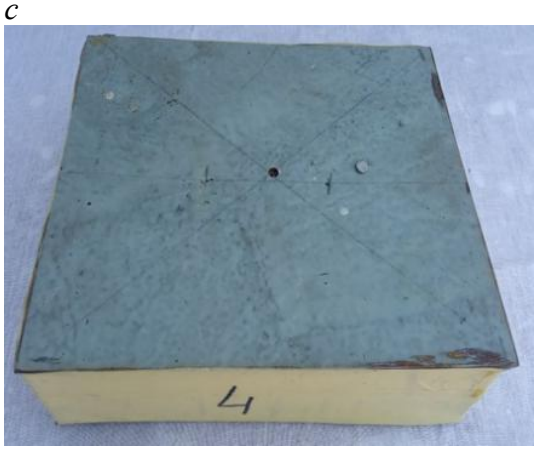

d

Fig. 5. – Prototypes of fencing: *a* – sample №2; *b* – sample №3; *c* – sample №3; *d* – sample №4

Experimental studies were carried out on the bench at a temperature of tamb 10 ˚C and – 10 °C. The main components in sample №2 are isomast, sealant and isover; in sample №3 - corundum, polyurethane foam and polyurethane foam; in sample №4 – corundum and polyurethane foam; in sample №5 – corundum, polyurethane foam and isover.

Each sample was tested continuously for 23-24 hours. The temperature in the test chamber was maintained so that the temperature difference in the chamber was 52 °C with an interval ± 0.5 °C. After completion of the tests, the results were processed and summarized in table 4.

Table 4 – Results of experimental tests of prototypes of fencing

Samples	Temperature differenceΔt °C	Heater on time τ, hour	Power consumption W, W h	Full chamber heat transfer coefficient K_f, W/m^2 K	Chamber body heat transfer coefficient K_{fr}, W/m^2 K	The coefficient of heat transfer of the lid (sample) theoretical K_{lid} teor	Experimental cover heat transfer coefficient K_{lid} exp, W/m2 K
2	51	18.5	241	0.490	0.482	0.520	0.502
3	52.5	20	235	0.470	0.482	0.329	0.340
4	51.5	20.5	240	0.472	0.482	0.384	0.364
5	52	20	219	0.473	0.482	0.385	0.370

Figure 9 shows a graph of temperature and power consumption during testing of four samples of thermal insulation.

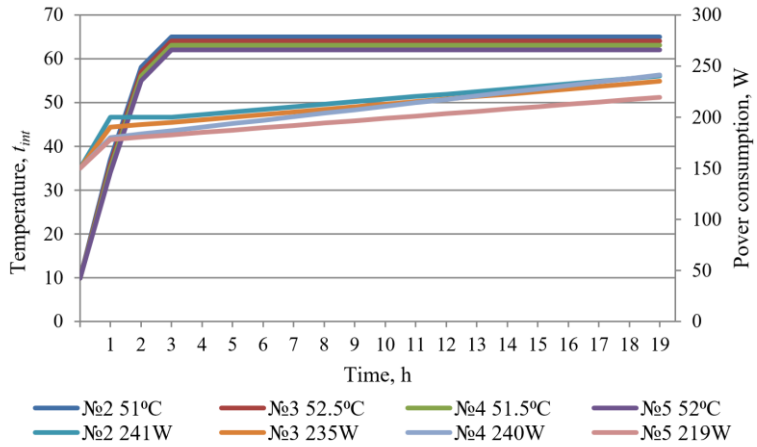

Fig. 9. – Diagram of change of temperature t_{inl} and power consumption W in relation to time of 2, 3, 4, 5 samples

After turning on the heater, the temperature increase continued for 1.5-2 hours until the temperature difference t_{int} - t_{ext} – 52 °C, an unsteady heat transfer mode occurred. Then came the steady state of heat transfer. For further calculations, the values of the steady-state heat transfer mode were taken.

As a result of experiments, based on the obtained experimental data, the heat transfer coefficients K_f of the test chamber with test samples were calculated using the formula

$$K_f = \frac{W}{F_f \cdot \tau \cdot (t_{int} - t_{ext})},$$

Further, according to the already known coefficients of the test chamber K_f, the body of the chamber K_{fr}, the heat transfer coefficient of the covers of samples number 2, 3, 4, 5 is determined by the formula

$$K_{lid} = \frac{K_f(F_{fr} + F_{lid}) - K_{fr} \cdot F_{fr}}{F_{lid}}$$

Calculation results are given in table 4. According to the data of table 4, a graph (figure 10) of changes in the heat transfer coefficient of samples № 2, 3, 4, 5 was plotted.

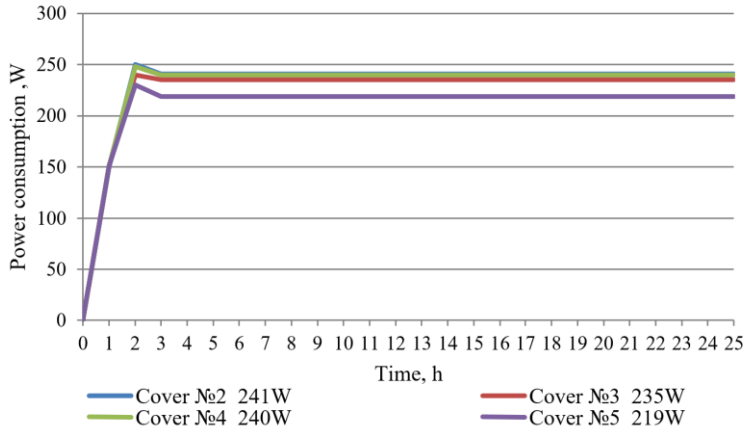

Fig. 10. – Diagram of electric power consumption *W* in the chamber

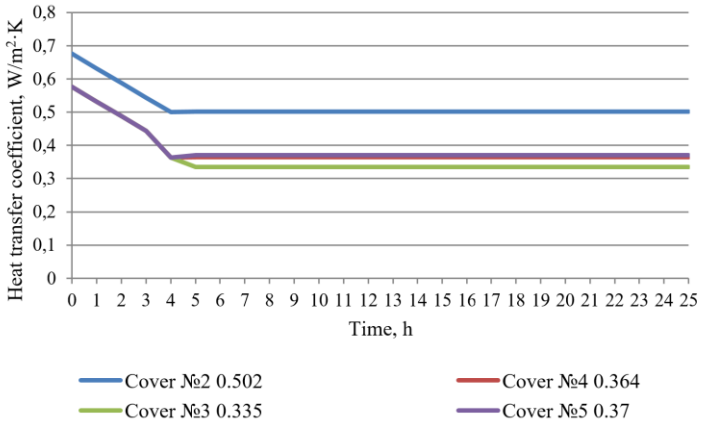

Fig. 11. – Diagram of change of heat transfer coefficient K_{lid} of test samples heat shielding in the chamber.

The heat transfer coefficient of the sample at low power consumption has a high value, then, as the temperature and power consumption increase, it normalizes and takes constant values.

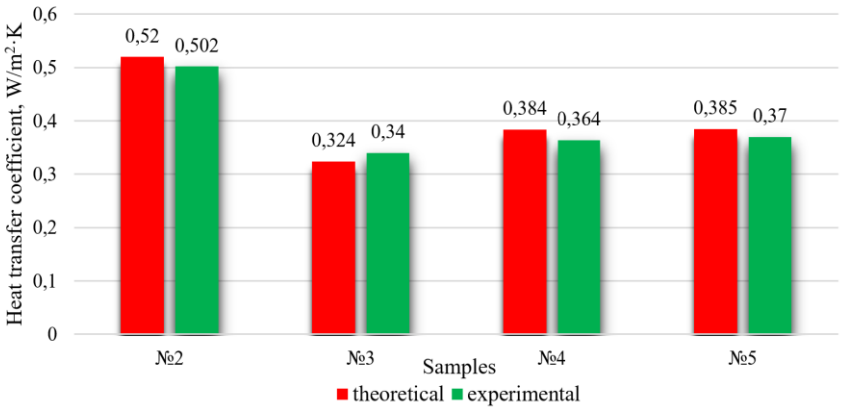

Fig. 12. – Bar chart of sample heat transfer coefficient values

According to experimental studies, it can be concluded that the highest heat transfer coefficient $K = 0.502$ W/m^2·K has sample № 2, in which isomast (bitumen resin, sealant and isover) is used as thermal insulation. Bituminous resin and sealant after drying become solid, susceptible to cracking and crevices. Isover is used in the form of bags made of film, which over time can crack and

condensate (moisture) penetrates into the bag, which reduces moisture resistance. As a result, condensate is formed under the inner skin, which flows down and corrosion of the lower sheets of the outer skin occurs. Thus, heat-insulating materials resin, sealant and isover are not recommended for use.

The best results were shown by samples №3 (K_3 = 0,340 W/m^2·K) and № 4 (K_4 = 0,364 W/m^2·K). Sample № 3 used corundum, polyurethane foam, and foamed plex, while sample № 4 used corundum and polyurethane foam having very low thermal conductivity coefficients. Corundum has a thermal conductivity of λ = 0,0012 W/m·K. This is a liquid material based on alkyd enamel, when thickened, it is easily diluted with water, easily applied with a brush or spray, reliably fills all looseness and crevices. It covers all metal elements of the body frame (sheathing sheets, vertical and horizontal elements), protecting them from corrosion. A layer of applied corundum 1-2.5 mm thick provides a lower heat transfer coefficient.

Polyurethane foam, the thermal conductivity of which is 0.4 W/m·K, creates a fairly dense layer of insulation, covers all leakages. When the niche is filled, the polyurethane foam swells. This must be taken into account when applying foam, so that there are no convex places.

Foam with a thermal conductivity of λ = 0,028 W/m^2·K is a very convenient material, it is easily cut, does not require a polyethylene film, does not perceive moisture.

The result of sample № 5 was K_5 = 0,370 W/m^2·K. In this sample, together with polyurethane foam, isover in plastic bags is used, and the disadvantages of isover in bags are described above.

Thus, for introduction into production, variants of samples №3 and №4 are recommended, which not only have a low heat transfer coefficient, but also protect the body from corrosion.

Heat shielding of the body from samples №3 and №4 with a thickness of 80 mm is quite suitable for the side walls. Solar radiation fully affects the roof of the car, so it is advisable to increase the thickness of the roof fence using the same materials

It is proposed to increase the roof fences to 110 mm due to the use of a wooden beam 50 mm thick. Then the thickness of the corundum layer will increase to 2 mm, polyurethane foam – 55 mm, foam plex – 50 mm.

The calculation of the heat transfer coefficient of the roof with a thickness of 110 mm according to was made using formula 4 and amounted to K_{lid} = 0.256 W/m^2·K. Such a value of the coefficient K_{lid} will reduce the heat flow penetrating inside the car.

After the completion of experimental work with samples of the body fence, an attempt was made to determine the heat transfer coefficient of the car body. The heat transfer coefficient of the car K_K body can be determined by the formula

$$K_{fr} \cdot F_{fr} = 2K_{sw} \cdot F_{sw} + K_{lid} \cdot F_{lid} + K_{face} \cdot F_{face},$$

where K_{sw}, K_{lid}, K_{bott}, K_{face} – heat transfer coefficients of body elements; F_{sw}, F_{lid}, F_{bott}, F_{face} – mean geometric areas of body elements.

Since the end parts of the car have two walls on each side of the car, their value (K_{face}·F_{face}) can be neglected in this case. The coefficients K_{sw} and K_{lid} can be taken from the obtained experimental data. The coefficient K is not defined in this study, it can be borrowed from studies [2-3]. K_{bott}≈0,5-0,55 W/m^2·K.

Based on the results of the preliminary calculation, we obtain that K_{int} = 0.6-0.65 W/m^2·K, which is 40% lower than known from V.V. Lukin [1] K_l = 1.0-1.1 W/m^2·K.

Finally, the heat transfer coefficient of the car can be determined after testing the car after construction with a fence made of the proposed materials.

Technical solutions based on research results. As a result of the theoretical and experimental studies carried out, the following technical solutions can be made:

1. For thermal insulation of passenger cars, it is recommended to use samples of thermal insulation №3 and 4. In sample №3, corundum, polyurethane foam and polyurethane foam are used as thermal insulation, which are easy to apply and have a large number of positive qualities. The value of the heat transfer coefficient of sample №3 according to theoretical calculations is K=0,329 W/m^2·K, and according to experimental data – K=0,340 W/m^2·K. The discrepancy was 3.3%.

In sample №4, corundum and polyurethane foam were used for thermal insulation. The heat transfer coefficient of sample №4 is equal to K=0,384 W/m^2 ·K according to theoretical calculations, and according to experimental data K=0,364 W/m^2·K. The discrepancy was 3.6%.

The thickness of samples №3 and №4 is assumed to be 80 mm, which will increase the internal width by 40 mm.

2. It is recommended to increase the thickness of the thermal roof fence to 110 mm for greater efficiency of protection against solar radiation.

3. To reduce the impact of solar radiation, paint the roof in light gray shades and, as an option, paint the roof with corundum anticorrosive.

Conclusions

The paper analyzed the existing thermal protection materials for fencing the car body with the lowest thermal conductivity coefficients and carried out appropriate tests. For experimental testing, 4 prototypes of the body fence were made, in which heat-shielding materials corundum, polyurethane foam, polyurethane foam and izover were used. Calibration of the test chamber made it possible to experimentally determine the heat transfer coefficient of the test chamber with three removable covers.

According to the improved methodology for conducting experimental studies of body fencing samples, the choice of thermotechnical materials for introduction into production is experimentally justified. Samples №3 and №4, which showed the lowest heat transfer coefficient – K_3=0,335 W/m^2·K and K_4=0,364 W/m^2·K are recommended for implementation in the production of passenger cars.

It is proposed to increase the thickness of the roof fence of the car to 110 mm to protect against solar radiation.

References

1. Lukin V.V. Wagons. General course. Textbook for railway transport universities / V.V. Lukin, P.S. Anisimov, Yu.P. Fedoseev. – M: Marshrut, 2004. – 424 p.

2. Djabbarov S., Saidivaliev S., Abdullayev B., Gayipov A., Rakhmatov K., Soboleva I. Study of the kinematic characteristics of the motion of the car from the top to the design point / E3S Web of Conferences. – International Scientific Siberian Transport Forum - TransSiberia 2023. – Vol. 402. – 04010. – pp. 1–14; DOI:10.1051/e3sconf/202340204010.

3. Khurmatov, Ya.A., Khaydarov, O.U., Abdullaev, B.A., Djabbarov, Sh.B., Inagamov, S.G. Evaluation of the efficiency of the friction tread brake of the diesel motor car / E3S Web of Conferences. – International Scientific Siberian Transport Forum - TransSiberia 2023. – Vol. 402. – 04009. – pp. 1–8; DOI: 10.1051/e3sconf/202340204009.

4. Inagamov S., Djabbarov S., Abdullaev B., Ruzmetov Ya., Inoyatov K., Hurmatov, Y. Study of the friction of the brake shoe of a freight car / E3S Web of Conferences. – V International Scientific Conference "Construction Mechanics, Hydraulics and Water Resources Engineering" (CONMECHYDRO - 2023) – Vol. 401. – 05036. – pp. 1–10; DOI: 10.1051/e3sconf/202340105036.

5. OST 33661–2015. Enclosing structures of railway rolling stock premises. Test methods for determining thermal performance with the Amendment. – M.: Standartinform, 2016. – 32 p.

6. Inoyatov, K., Abdullaev, B., Rakhmatov, K. Impact of solar radiation on the climate of a passenger car / E3S Web of Conferences. – International Scientific Conference on Biotechnology and Food Technology (BFT-2023) – Vol. 460. – 07015. – pp. 1–7; DOI: 10.1051/e3sconf/202346007015.

7. Djabbarov, S., Saidivaliev, S., Abdullaev, B., Ortiqov, M., Rustamov, N. Mathematical model of wagon wheels rolling along the hump profile. Simulation of movements of cargo with a flat base on a four-axle platform. E3S Web of Conferences. – International Scientific Conference on Biotechnology and Food Technology (BFT-2023) – Vol. 460. – 06007. – pp. 1–17; DOI: 10.1051/e3sconf/202346006007.

8. Saidivaliev, S., Djabbarov, S., Abdullaev, B., Ortiqov, M., Rustamov, N. Simulation of movements of cargo with a flat base on a four-axle platform / E3S Web of Conferences. – International Scientific Conference on Biotechnology and Food Technology (BFT-2023) – Vol. 460. – 06008. – pp. 1–12; DOI: 10.1051/e3sconf/202346006008.

9. Kitaev B.N. Heat exchange processes during the operation of wagons. M., Transport. 1984. 184p.

10. Starikov A.P., Kuzmenko D.Yu. Development of criteria for assessing the effectiveness of heat conservation by enclosing structures of passenger cars. OGUPT. UDC 629.45:629.4.016.15. - P. 69-72.